

Article

Electrophoresis of Two Identical Rigid Spheres in a Charged Cylindrical Pore

Jyh-Ping Hsu, and Li-Hsien Yeh

J. Phys. Chem. B, **2007**, 111 (10), 2579-2586 • DOI: 10.1021/jp068407z

Downloaded from <http://pubs.acs.org> on November 18, 2008

More About This Article

Additional resources and features associated with this article are available within the HTML version:

- Supporting Information
- Links to the 1 articles that cite this article, as of the time of this article download
- Access to high resolution figures
- Links to articles and content related to this article
- Copyright permission to reproduce figures and/or text from this article

[View the Full Text HTML](#)



ACS Publications
High quality. High impact.

Electrophoresis of Two Identical Rigid Spheres in a Charged Cylindrical Pore

Jyh-Ping Hsu* and Li-Hsien Yeh

Department of Chemical Engineering, National Taiwan University, Taipei 10617, Taiwan

Received: December 6, 2006; In Final Form: January 18, 2007

The electrophoresis of two identical spheres moving along the axis of a long cylindrical pore under the conditions of low surface potential and weak applied electric field is investigated. The geometry considered allows us to examine simultaneously the effects of boundary and the presence of a nearby entity on the behavior of a particle. The influences of the separation distance between two spheres, the thickness of a double layer, the ratio (radius of sphere/radius of pore), and the charged conditions on the surfaces of the spheres and the pore on the mobility of a particle are investigated. Several interesting results that are not reported in the literature are observed. For instance, although for the case of two positively charged spheres in an uncharged pore the qualitative behavior of a sphere depends largely on its size relative to that of a pore and the thickness of the double layer, this might not be the case when two uncharged spheres are in a positively charged pore. In addition, in the latter, the mobility of a sphere increases with the increases in the separation distance between two spheres, and this effect is pronounced when the ratio (radius of sphere/radius of pore) takes a medium value or the thickness of the double layer is either sufficiently thin or sufficiently thick.

1. Introduction

Electrophoresis, one of the electrokinetic phenomena, is of both fundamental and practical significance. Although its principle is straightforward, solving an electrophoresis problem under general conditions is extremely difficult, if not impossible, and available theoretical results in the literature are mainly based on drastic assumptions. Often, two major effects need to be considered in practice; namely, the presence of a boundary and the influence of nearby particles. The former is important when electrophoresis is conducted in a small space, such as capillary electrophoresis and electrophoresis through a porous medium. The latter should not be neglected when the concentration of particles is appreciable.

Previous analyses revealed that the presence of a boundary can have a profound influence on the electrophoretic behavior of a particle. In general, it will influence the viscous drag on a particle, distort the local electric field near particle surface, and induce an electroosmotic flow or an osmotic pressure field or both. These lead to some interesting observations. In the electrophoresis of a sphere parallel to a plane,¹ for instance, it was predicted that for moderate to large separations between particle and plane, the presence of the latter has the effect of reducing the electrophoretic mobility of the former, but the reverse is true if they are sufficiently close to each other. In a study of the electrophoresis of a charged-regulated sphere normal to a large disk, Hsu et al.² showed that the electrophoretic mobility of a sphere could have a local maximum as the double layer thickness or the separation distance between them varies; the direction of the movement of a sphere might also change. For the electrophoresis of a sphere along the axis of a cylindrical pore,³ if the former is uncharged and the latter positively charged, or if both of them are positively charged, the absolute value of the mobility of a sphere could have a local maximum as the thickness of the double layer varies.

The presence of nearby particles can also have an important influence on the electrophoretic behavior of a particle. For example, in a study of the electrophoresis of two spheres in an infinite medium, Shugai et al.⁴ concluded that the effect of particle–particle interaction can be significant if the thickness of the double layer surrounding a sphere is comparable to its radius. A similar conclusion was also made by Hsu et al.⁵ in an analysis of the electrophoresis of two cylindrical particles with constant charge density along the axis of a cylindrical pore. Several other efforts have been made to interpret the influence of nearby particles on the electrophoretic behavior of a particle. These include, for instance, the electrophoresis of two spheres in an infinite medium^{6–9} and the electrophoresis of multiple spheres in an infinite medium.^{10–13} In general, the thickness of the double layer and the separation distance between two particles play the major roles.

In this study, the effects of particle–particle interaction and particle–boundary interaction on the electrophoretic behavior of a particle are investigated simultaneously by considering the electrophoresis of two identical spheres along the axis of a cylindrical pore under the conditions of low surface potential and weak applied electric field. In particular, the wall of a pore can be either uncharged, such as a fused-silica pore coated with a hydrophobic polymer, or charged, such as a fused-silica pore. In the latter, an electroosmotic flow is present, and the phenomenon under consideration becomes much more complicated than that in the former.

2. Theory

As Shown in Figure 1, we consider the electrophoresis of two identical, rigid, nonconducting, spherical particles of radius a along the axis of an infinite, nonconducting cylindrical pore of radius b . Let $2h$ be the center-to-center distance between two spheres. The cylindrical coordinates (r, θ, z) are chosen with its origin located at the center of one of the two spheres, and a uniform electric \mathbf{E} , which is in the z -direction when strength E is applied. Since the geometry under consideration is θ -sym-

* Corresponding author. Tel: 886-2-23637448. Fax: 886-2-23623040. E-mail: jphsu@ntu.edu.tw.

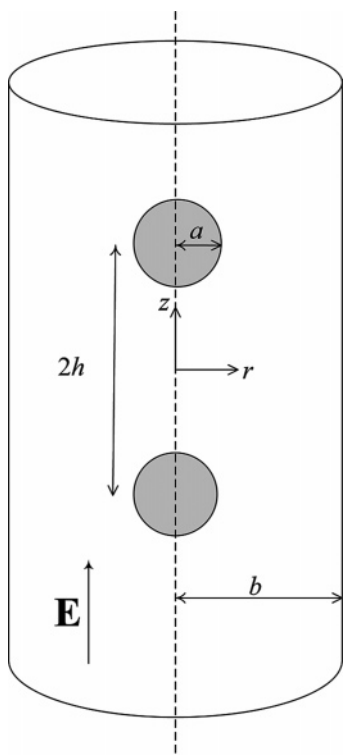


Figure 1. Schematic representation of the problem considered in which two identical spheres of radius a with a center-to-center distance $2h$ are placed on the axis of an infinite cylindrical pore of radius b . A uniform applied electric field \mathbf{E} parallel to the axis of the pore is applied. The cylindrical coordinates (r, θ, z) with its origin located at the center of one of the spheres are chosen.

metric, only the (r, z) domain need to be considered. Suppose that the spatial variation of the electrical potential Ψ can be described by the Poisson–Boltzmann equation

$$\nabla^2 \Psi = -\frac{\rho_e}{\epsilon} = -\frac{\sum_{j=1}^N z_j e n_j^0 \exp(-z_j e \Psi / k_B T)}{\epsilon} \quad (1)$$

In this expression, ∇^2 is the Laplace operator; ϵ is the permittivity of the liquid phase; ρ_e is the space charge density; N is the number of ionic species; n_j^0 and z_j are the bulk number concentration and the valence of ionic species j , respectively; and e , k_B , and T are the elementary charge, the Boltzmann constant, and the absolute temperature, respectively. If \mathbf{E} is weak relative to the electric field established by the spheres and the pore and the surface potential is low, then the effect of double layer polarization can be neglected. In this case, Ψ can be expressed as the sum of the equilibrium potential Ψ_1 ; the potential in the absence of \mathbf{E} ; and a perturbed potential Ψ_2 , which arises from \mathbf{E} .¹⁴ Since the surface potential is low, these potentials can be described by

$$\nabla^2 \Psi_1 = \kappa^2 \Psi_1 \quad (2)$$

$$\nabla^2 \Psi_2 = 0 \quad (3)$$

where $\kappa = [\sum_j n_j^0 (e z_j)^2 / \epsilon k_B T]^{1/2}$ is the reciprocal Debye length. Since the spheres and the pore are nonconductive and remained at constant surface potentials, ζ_p and ζ_w , respectively, the boundary conditions associated with eqs 2 and 3 are

$$\Psi_1 = \zeta_p \quad \text{and} \quad \mathbf{n} \cdot \nabla \Psi_2 = 0 \quad \text{on the particle surface} \quad (4)$$

$$\Psi_1 = \zeta_w \quad \text{and} \quad \frac{\partial \Psi_2}{\partial r} = 0, \quad r = b \quad (5)$$

$$\Psi_1 = \zeta_w \frac{I_0(\kappa r)}{I_0(\kappa b)} \quad \text{and} \quad \nabla \Psi_2 = -\mathbf{E} \quad \text{for } |z| \rightarrow \infty, r < b \quad (6)$$

In these expressions, \mathbf{n} is the unit outward normal vector, and I_0 is the modified Bessel function of the first kind of order zero.

The flow field in electrophoresis is in the creeping flow regime. At steady state, we have

$$\nabla \cdot \mathbf{u} = 0 \quad (7)$$

$$\eta \nabla^2 \mathbf{u} - \nabla p = \rho_e \nabla \Psi_2 \quad (8)$$

In these expressions, \mathbf{u} , η , and p are, respectively, the velocity, the viscosity, and the pressure of the liquid phase, and $\rho_e \nabla \Psi_2$ is the electric body force acting on the fluid. We assume the following boundary conditions:

$$\mathbf{u} = U \mathbf{e}_z \quad \text{on particle surface} \quad (9)$$

$$\mathbf{u} = 0, \quad r = b \quad (10)$$

$$\mathbf{u} = u(r) \mathbf{e}_z = -\frac{\epsilon \zeta_w}{\eta} \left[1 - \frac{I_0(\kappa r)}{I_0(\kappa b)} \right] \mathbf{E} \mathbf{e}_z, \quad |z| \rightarrow \infty, r < b \quad (11)$$

In these expressions, U is the particle velocity in the z -direction, \mathbf{e}_z is the unit vector in the z -direction, and $u(r)$ is the undisturbed electroosmotic velocity in a long cylindrical pore with surface potential ζ_w when the spheres are absent. Equations 9 and 10 imply that both the surface of a sphere and that of a pore are no-slip.

The forces acting on a sphere include the electrostatic force and the hydrodynamic force. For the present case, only the z -components of these forces need to be considered. The z -component of the electrostatic force, F_E , can be calculated by^{4,15–17}

$$F_E = \int \int_S \sigma_p E_z dS \quad (12)$$

where S denotes the surface of a sphere, $\sigma_p = -\epsilon \mathbf{n} \cdot \nabla \Psi_1$ is the surface charge density, and $E_z = -\partial \Psi_2 / \partial z$ is the strength of the local external electric field in the z -direction. The hydrodynamic force acting on a sphere in the z -direction, F_D , can be evaluated by¹⁸

$$F_D = \int \int_S \eta \frac{\partial(\mathbf{u} \cdot \mathbf{t})}{\partial n} t_z dS + \int \int_S -p n_z dS \quad (13)$$

where \mathbf{t} is the unit tangential vector on S , n is the magnitude of \mathbf{n} , and t_z and n_z are the z components of \mathbf{t} and \mathbf{n} , respectively. Although U can be estimated on the basis of the condition that $(F_E + F_D)$ vanishes at a steady state through a trial-and-error procedure, a more efficient approach is applicable for the present case in which the problem is mathematically decomposed into two subproblems.¹⁹ In the first subproblem, both spheres move with U in the absence of \mathbf{E} , and in the second subproblem, \mathbf{E} is applied, but both spheres remain fixed. In the former, a sphere experiences a conventional hydrodynamic drag, $F_{D,1} = -UD$, where the drag coefficient, D , is positive and depends upon the considered geometry. In the latter, both an electrostatic force F_E and a hydrodynamic force $F_{D,2}$ act on a sphere, where $F_{D,2}$ arises from the movement of the mobile ions in an electric

double layer. Both F_E and $F_{D,2}$ are functions of κa , (h/a) , and λ ; $F_{D,1}$ (or D) is a function of (h/a) and λ , but is independent of κa . Applying the relations $F_D = F_{D,1} + F_{D,2}$ and $F_{D,1} = -UD$, it can be shown that $F_E + F_D = 0$ leads to

$$U = \frac{F_E + F_{D,2}}{D} \quad (14)$$

Applying the procedure used previously,²⁰ U can be obtained. If we define $F_E^* = F_E/6\pi\eta a U_{\text{ref}}$, $F_{D,2}^* = F_{D,2}/6\pi\eta a U_{\text{ref}}$, and $D^* = D/6\pi\eta a$, then eq 14 can be rewritten as

$$U^* = \frac{F_E^* + F_{D,2}^*}{D^*} \quad (15)$$

where $U^* = U/U_{\text{ref}}$ is the scaled electrophoretic mobility, with $U_{\text{ref}} = \epsilon\zeta_{\text{ref}}E/\eta$ and $\zeta_{\text{ref}} = k_B T/e$.

The governing equations for the electrical and the flow fields are solved numerically considering the assumed boundary conditions. To this end, FlexPDE,²¹ a differential equation solver based on a finite element method, is chosen. The applicability and the accuracy of this software were justified previously³ and will also be discussed later.

3. Results and Discussion

We consider two representative cases: two positively charged spheres with a scaled constant surface potential $\zeta_p^* = e\zeta_p/k_B T = 1$ are placed in an uncharged pore, and two uncharged spheres are placed in a positively charged pore with a scaled constant surface potential $\zeta_w^* = e\zeta_w/k_B T = 1$. Since the problem under consideration is of a linear nature, the results for the case when both the spheres and the pore are positively charged can be obtained by summing the results from the above two cases.

3.1. Positively Charged Spheres in Uncharged Pore. Let us consider first the case when two positively charged spheres are placed in an uncharged pore. It is known that under creeping flow conditions, the hydrodynamic forces exerted on two identical spheres are the same.^{22,23} In addition, under the same external force field, two spheres move faster than one isolated sphere.^{22,23} Shugai et al.⁴ showed that the electrophoretic mobilities of two neighboring spheres are the same. Figure 2 shows the variation of D^* and U^* as a function of (h/a) at various λ 's when the radius of a sphere, a , is fixed. Figure 2a suggests that for a fixed λ , D^* increases with the increase in (h/a) and approaches a constant value, which is the result for the case when only one sphere is present in a pore. This is because the smaller the (h/a) , the closer the spheres and the stronger the interaction between them. Figure 2a also indicates that if (h/a) is fixed, D^* increases with the increase in λ . This is because the larger the λ , the more significant the presence of the boundary (pore wall), which has the effect of retarding the movement of a sphere. Note that if $h/a \rightarrow 0$ and $\lambda \rightarrow 0$, then $D^* \rightarrow 0.645$, as predicted by Stimson and Jeffery.²² D^* is found to depend weakly on (h/a) , except when λ is sufficiently small (<0.5). As can be seen in Figure 2b, if λ is small, U^* declines with the increase in (h/a) and approaches a constant value, which is the result for the electrophoresis of a sphere along the axis of a cylindrical pore; however, if λ exceeds about 0.4, U^* increases with the increase in (h/a) . The former can be inferred from similar analyses in the literature;^{4,5} the latter has never been reported. This is because as (h/a) increases, the rate of increase of D^* is always faster than that of the scaled net driving force ($F_E^* + F_{D,2}^*$) if λ is small, but the reverse is true if λ is large. Note that U^* is insensitive to the variation of (h/a) , except

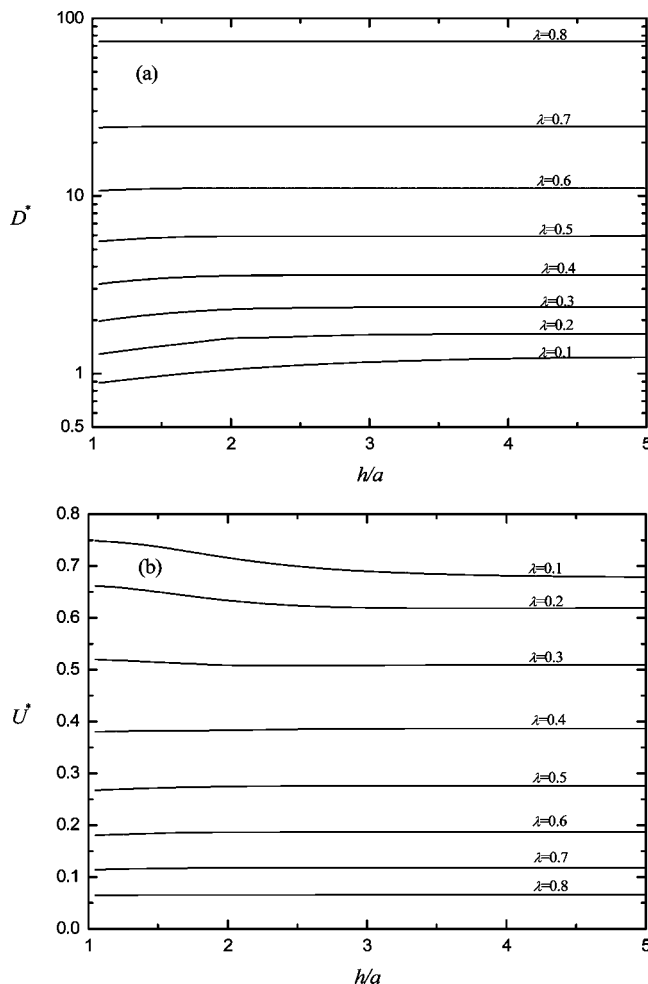


Figure 2. Variation of the scaled hydrodynamic force coefficient D^* (a) and the scaled electrophoretic mobility, U^* , (b) as a function of (h/a) at various values of λ for the case when two spheres are positively charged and the pore is uncharged. Key: $\zeta_p^* = 1$, $\zeta_w^* = 0$, and $\kappa a = 1$.

when λ is sufficiently small (<0.4), which implies that if λ is large, the viscous drag arising from the presence of the pore dominates. Similar behavior was also observed in the electrophoresis of two identical cylindrical particles with a constant charge density along the axis of a cylindrical pore.⁵ The variations of F_E^* , $F_{D,2}^*$, and $(F_E^* + F_{D,2}^*)$ as a function of (h/a) at various values of λ for the case of Figure 2 are illustrated in Figure 3. F_E^* is found to increase with the increase in λ or increase with the increase in (h/a) and approaches a constant value, which is the result for the case when only one sphere is present in the pore. The latter is because the smaller the (h/a) , the closer the spheres and the greater the amount of negative charge induced on their surfaces, which has the effect of reducing the surface charge density of the spheres. The former is a consequence of the combined effect of the squeeze of the applied electric field between the spheres and the pore and the increase in the surface charge density as λ increases.²⁰ On the basis of eq 13, $F_{D,2}^*$ can be expressed as $F_{D,2}^* = F_{D,2(v)}^* + F_{D,2(p)}^*$, that is, the sum of a viscous term and a pressure term. Figure 3a reveals that if λ is small (boundary effect is unimportant), $F_{D,2}^*$ is a retardation force, but it becomes a driving force when λ is large. The latter arises because the pressure term dominates.²⁰ Figure 3a also indicates that $F_{D,2}^*$ has a local minimum as (h/a) varies, which is more pronounced when λ is small, and the value of (h/a) at which the local minimum of $F_{D,2}^*$ occurs decreases with the increase in λ . The observation that $|F_{D,2}^*|$

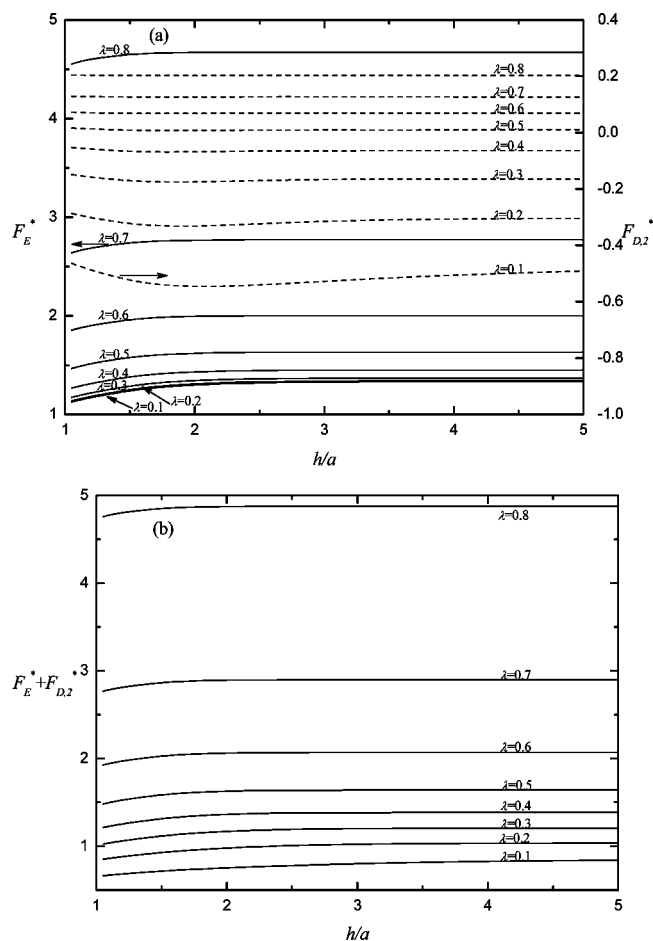


Figure 3. Variation of the scaled electrostatic force, F_E^* , and the scaled excess hydrodynamic force, $F_{D,2}^*$ (a), and the scaled net driving force, $(F_E^* + F_{D,2}^*)$ (b), as a function of (h/a) at various values of λ for the case of Figure 2.

declines with the decrease in (h/a) when two spheres are sufficiently close to each other arises from the competition between $F_{D,2(v)}^*$ and $F_{D,2(p)}^*$ as (h/a) varies. For example, if $\lambda = 0.1$, with less boundary effect, $F_{D,2}^*$ is mainly dominated by $F_{D,2(v)}^*$. As (h/a) decreases, the spheres experience a relative large $|F_{D,2}^*|$ arising from the interaction of the flow field near a sphere with that near the other one, which enhances the electroosmotic flow surrounding them and raises the magnitude of $|F_{D,2(v)}^*|$. If (h/a) is sufficiently small, because the electroosmotic flow is reduced by the increase of the amount of negative induced charge due to the overlapping of the electric double layers, $|F_{D,2}^*|$ begins to decline with the increase in (h/a) . It is interesting to note that $F_{D,2}^*$ depends weakly on (h/a) , except when λ is sufficiently small (<0.4). This is because $F_{D,2(p)}^*$ is larger than $|F_{D,2(v)}^*|$, and it depends weakly on (h/a) when λ is sufficiently large due to the hindrance of the pore wall. Figure 3b shows that $(F_E^* + F_{D,2}^*)$ increases with the increase in (h/a) and approaches a constant value, which is the result for the case when only one particle is present in the pore. In addition, for a fixed value of (h/a) , $(F_E^* + F_{D,2}^*)$ increases with the increase in λ . The behavior of $(F_E^* + F_{D,2}^*)$ as (h/a) varies is similar to that of F_E^* seen in Figure 3a, implying that F_E^* is the main driving force.

Figure 4 shows the variation of U^* as a function of (h/a) at various κa for the case when $\lambda = 0.4$, and the corresponding variations of F_E^* , $F_{D,2}^*$, and $(F_E^* + F_{D,2}^*)$ are presented in Figure 5. Here, a is fixed and κ varies; that is, the radius of a sphere is

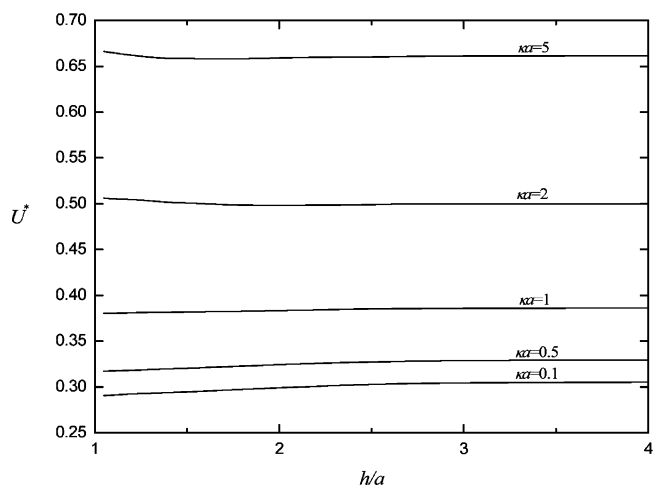


Figure 4. Variation of the scaled electrophoretic mobility, U^* , as a function of (h/a) at various values of κa . Key: $\zeta_p^* = 1$, $\zeta_w^* = 0$, and $\lambda = 0.4$.

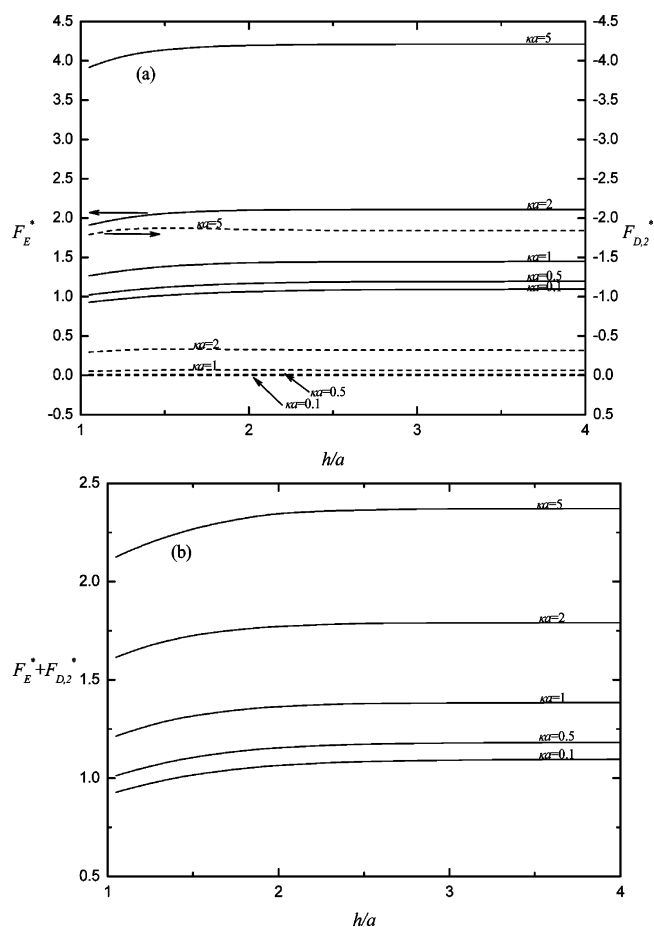


Figure 5. Variation of the scaled electrostatic force, F_E^* , and the scaled excess hydrodynamic force, $F_{D,2}^*$ (a), and the scaled net driving force, $(F_E^* + F_{D,2}^*)$ (b), as a function of (h/a) at various values of κa for the case of Figure 4.

fixed and the electrolyte concentration varies. Figure 4 reveals that if κa is small (thicker double layer), U^* increases with the increase in (h/a) and approaches a constant value, which is the result for the case when only a sphere is present in the pore. However, as κa becomes large, U^* declines with the increase in (h/a) , and if it is sufficiently large, U^* has a local minimum. These phenomena have never been reported in the literature. It is interesting to note that the local minimum appears only if κa

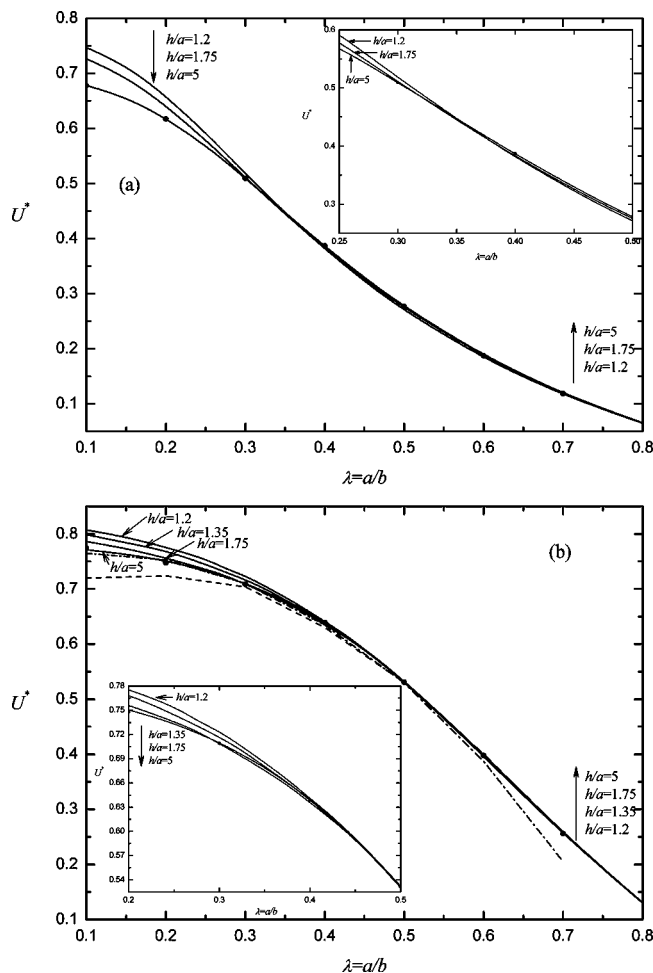


Figure 6. Variation of the scaled electrophoretic mobility, U^* , as a function of λ at various values of (h/a) . (a) $\kappa a = 1$, (b) $\kappa a = 4.3$. Discrete symbols, Hsu et al.;³ dashed line, results of Shugai and Carnie;¹⁵ dashed-dotted line, Ennis and Anderson;²⁴ solid line, present study. Parameters used are $\zeta_p^* = 1$ and $\zeta_w^* = 0$.

is sufficiently large; for instance, it does not show in Figure 2b, where $\kappa a = 1$. The specific behaviors of U^* as κa becomes large can be explained thus: as (h/a) increases, the rate of increase of $(F_E^* + F_{D,2}^*)$ is always faster than that of D^* if κa is small (or λ is large). On the other hand, if κa sufficiently large (> 1), the rate of increase of D^* becomes faster than that of $(F_E^* + F_{D,2}^*)$ if (h/a) is small, but the reverse is true if it is large. Figure 4 also suggests that the smaller the κa , the smaller the U^* , and the larger the value of (h/a) for U^* to reach a constant value.

A similar phenomenon was also observed for the electrophoresis of two identical cylindrical particles with a constant charge density along the axis of a cylindrical pore.⁵ The former is because the thinner the double layer surrounding a sphere, the higher the charge density on its surface; the latter is because the thicker the double layer, the larger the separation distance between two spheres that is required to avoid double layer interaction. For a fixed value of κa , the qualitative behaviors of F_E^* , $F_{D,2}^*$ and $(F_E^* + F_{D,2}^*)$ seen in Figure 5 are similar to those presented in Figure 3. In addition, as expected, F_E^* , $F_{D,2}^*$, and $(F_E^* + F_{D,2}^*)$ all increase with the increase in κa .

Figure 6 shows the variation of U^* as a function of λ at various combinations of (h/a) and κa . For comparison, the results of Hsu et al.,³ Ennis and Anderson,²⁴ and Shugai and Carnie,¹⁵ all for the case when one sphere is in a cylindrical pore, are

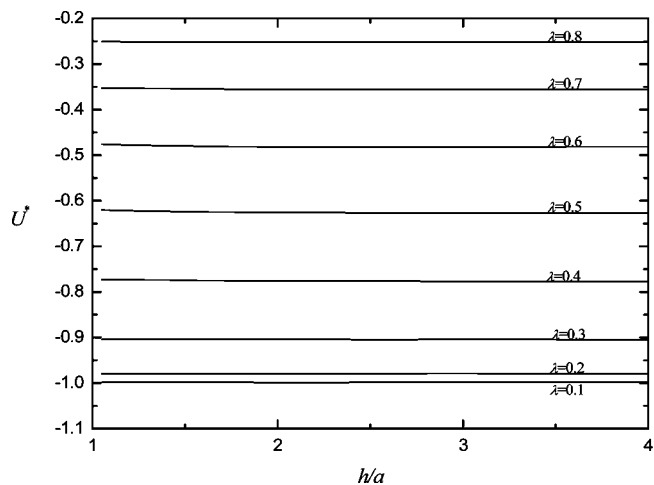


Figure 7. Variation of the scaled electrophoretic mobility, U^* , as a function of (h/a) at various values of λ for the case when two spheres are uncharged and the pore is positively charged. Parameters used are $\zeta_p^* = 0$, $\zeta_w^* = 1$, and $\kappa a = 1$.

also presented. Due to the methods adopted, the results of Shugai and Carnie¹⁵ are limited to a sufficiently large λ , and those of Ennis and Anderson²⁴ are limited to a sufficiently small λ . In contrast, the present approach does not have these limitations, and its performance seems to be satisfactory for the range of λ considered, as is justified by that the present results approach those of Hsu et al.³ as (h/a) increases. Figure 6 reveals that if λ is small, the smaller the (h/a) , the larger the U^* , but the reverse is true if λ is large. This implies that if λ is small, the U^* for the case of two spheres is larger than that for the case of one sphere, but the reverse is true if λ is large. The general trends of U^* as (h/a) varies are consistent with the results shown in Figure 2b. Note that if λ takes a medium value in Figure 6b, where $\kappa a = 4.3$, U^* has a local maximum as (h/a) varies. The general trends of U^* as (h/a) varies for a sufficiently large κa are also consistent with the results shown in Figure 4. As can be seen in Figure 6, the critical value of λ , λ_c , at which the qualitative trend of U^* as (h/a) varies depends largely upon the values of κa , (h/a) , and λ . In general, for a fixed value of κa , λ_c declines with an increase in (h/a) . Again, these arise from the competition between $(F_E^* + F_{D,2}^*)$ and D^* and the sphere–sphere and sphere–pore interactions, which make the phenomenon under consideration more complicated than that for the cases when the pore is absent.⁴

3.2. Uncharged Spheres in Positively Charged Pore. Figure 7 shows the variation of U^* as a function of (h/a) at various values of λ when $\kappa a = 1$ for the case when two uncharged spheres are placed in a positively charged pore. The general qualitative behavior of U^* shown in this figure is similar to that seen in Figure 2b, except that U^* is negative for the ranges of the parameters considered. As will be illustrated later, the negative mobility arises from both the driving forces F_E^* and $F_{D,2}^*$ being negative. For a fixed value of λ , $|U^*|$ increases slightly with the increase in (h/a) and approaches a constant value, which is the result for the case when only a sphere is present. The increase in $|U^*|$ as (h/a) increases arises from the rate of increase of $(F_E^* + F_{D,2}^*)$ being always faster than that of D^* . Note that U^* is less sensitive to the variation in (h/a) when λ is small than when it is large, which is different from that shown in Figure 2b, where the spheres are positively charged and the pore is uncharged. For example, if $\kappa a = 1$, the maximum differences of $|U^*|$ from that for the case of an isolated sphere in a pore are 1.303, 0.566, and 0.037% for $\lambda = 0.6, 0.4,$ and

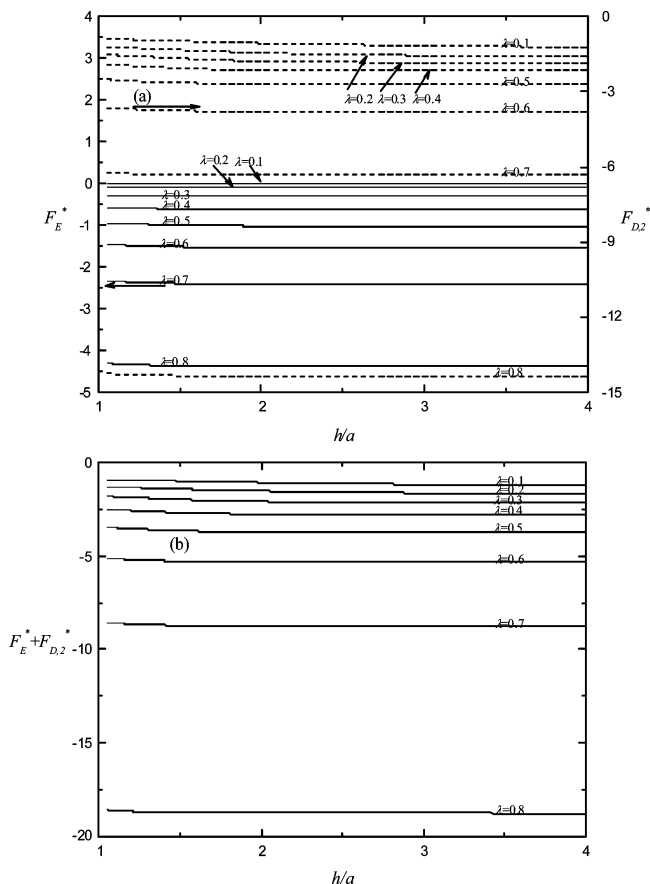


Figure 8. Variation of the scaled electrostatic force, F_E^* , and the scaled excess hydrodynamic force, $F_{D,2}^*$ (a), and the scaled net driving force, $(F_E^* + F_{D,2}^*)$ (b), as a function of (h/a) at various values of λ for the case of Figure 7.

0.1, respectively. The phenomena that for a fixed value of λ , $|U^*|$ increases slightly with an increase in (h/a) and U^* is less sensitive to the variation in (h/a) when λ is small than when it is large have never been reported in the literature. The latter can be explained by that when the boundary effect is unimportant, the interaction between two uncharged spheres is insignificant. Figure 7 also reveals that for a fixed (h/a) , U^* decreases rapidly with an increase in λ . Similar behavior is also observed for a sphere³ and a finite cylinder²⁰ in a cylindrical pore. This is because the undisturbed electroosmotic velocity $u(r)$ described by eq 11 is the main driving force for the movement of a sphere, and as λ (or κb) increases, the overlapping between the spheres and the double layer near the pore wall leads to a drastic decline in $u(r)$, as is justified by the behaviors of F_E^* , $F_{D,2}^*$, and $(F_E^* + F_{D,2}^*)$ presented in Figure 8. Figure 8a indicates that the qualitative behaviors of $|F_E^*|$ are similar to those of F_E^* shown in Figure 3a for the case when two spheres are positively charged and a pore is uncharged, and can be explained by the same reasoning. Note that F_E^* is negative because a negative charge is induced on the surfaces of the spheres as they approach the positively charged pore wall. If λ is sufficiently small (<0.3), the amount of induced charge decreases rapidly and vanishes as $\lambda \rightarrow 0$, so is $|F_E^*|$. This is consistent with the result of Hsu and Ku for the electrophoresis of a finite cylinder along the axis of a cylindrical pore.²⁰ As can be seen in Figure 8a, $|F_{D,2}^*|$ increases with the increase in (h/a) and approaches a constant value, and it increases with the increase in λ . The former is because the smaller the (h/a) , the stronger the interaction between the flow fields near the spheres, which has the effect

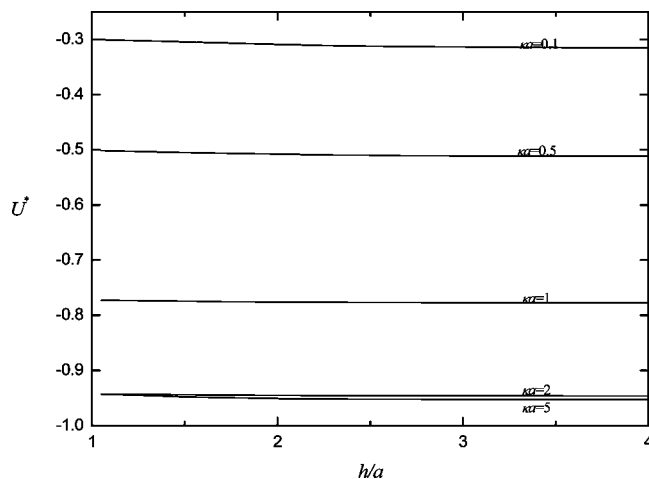


Figure 9. Variation of the scaled electrophoretic mobility, U^* , as a function of (h/a) for various values of κa at $\zeta_p^* = 0$, $\zeta_w^* = 1$, and $\lambda = 0.4$.

of decreasing the drag on a sphere. The latter is because the larger the λ , the more significant the presence of the pore wall, which has the effect of increasing the drag on a sphere. The qualitative behaviors of $|F_{D,2}^*|$ are similar to those of D^* shown in Figure 2a, although $F_{D,2}^*$ is acting as a driving force for the movement of a sphere. However, the qualitative behaviors of $F_{D,2}^*$ shown in Figure 8a are different from those illustrated in Figure 3a for the case when two positively charged spheres are placed in an uncharged pore where $F_{D,2}^*$ may change from negative to positive as λ increases. Figure 8b indicates that $|F_E^* + F_{D,2}^*|$ increases with the increase in (h/a) and approaches a constant value, and it increases with the increase in λ . These are expected.

The variation of U^* as a function of (h/a) at various κa 's for the case when $\lambda = 0.4$ are illustrated in Figure 9, and the corresponding variations of F_E^* , $F_{D,2}^*$, and $(F_E^* + F_{D,2}^*)$ are presented in Figure 10. The former indicates that if κa is fixed, $|U^*|$ increases slightly with the increase in (h/a) and approaches a constant value, which is consistent with the results shown in Figure 7 and can be explained by the same reasoning. As can be seen in Figure 10a, for a fixed κa , both $|F_E^*|$ and $|F_{D,2}^*|$ increase with the increase in (h/a) and approach a constant value, which is consistent with the result shown in Figure 8a and can be explained by the same reasoning. Figure 10a also indicates that $|F_E^*|$ decreases with the increase in κa , which is contrary to the behavior of F_E^* seen in Figure 5a, but $|F_{D,2}^*|$ increases with the increase in κa . The former is because a negative charge is induced on the surfaces of the spheres as they approach the positively charged pore. Note that if κa is sufficiently large, the amount of induced charge becomes insignificant, so is $|F_E^*|$. As pointed out by Hsu and Ku,²⁰ the latter is because if κa is not large enough, the undisturbed electroosmotic velocity $u(r)$ described by eq 11 increases rapidly with the increase in κa , so is $|F_{D,2}^*|$. Figure 10b suggests that $|F_E^* + F_{D,2}^*|$ increases with the increase in (h/a) and approaches a constant value, and it increases with the increase in λ . These are expected.

The influence of λ and κa on the behavior of U^* at various values of (h/a) is illustrated in Figure 11. This figure reveals that, for a fixed value of λ (or κa), the $|U^*|$ for the case of two spheres is smaller than that for the case of one sphere. This behavior is different from that for the case when two positively charged spheres are in an uncharged cylindrical pore shown in Figure 6 and has never been reported in the literature. Figure 11b suggests that if both λ and (h/a) are fixed, $|U^*|$ has a local

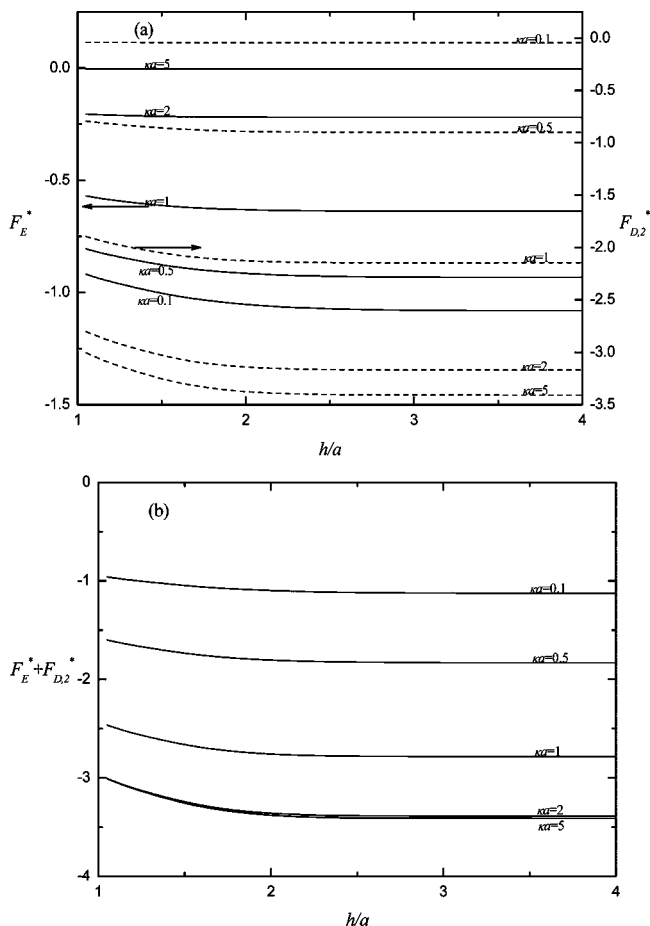


Figure 10. Variation of the scaled electrostatic force, F_E^* , and the scaled excess hydrodynamic force, $F_{D,2}^*$ (a), and the scaled net driving force, $(F_E^* + F_{D,2}^*)$ (b), as a function of (h/a) at various values of ka for the case of Figure 9.

maximum as ka varies. A similar phenomenon was also reported for the case when a sphere³ or a finite cylinder²⁰ is placed in a cylindrical pore. The presence of the local maximum arises from the net result of two competing driving forces as ka varies; namely, $|F_E^*|$ decreases with the increase in ka , but $|F_{D,2}^*|$ increases with the increase in ka , as shown in Figure 10a. In general, U^* is sensitive to the variation of (h/a) only if λ takes a moderate value or ka is either sufficiently large or sufficiently small. This phenomenon has not been reported in the literature. The former can be explained by that if λ is large, the viscous drag arising from the pore wall dominates; on the other hand, if λ is small, the overlapping between the spheres and the double layer of the pore is unimportant. The latter can be explained by that if ka is small, a larger separation distance between two spheres is required to avoid double layer interaction. On the other hand, if ka is large, U^* is dominated by $F_{D,2}^*$, which is sensitive to the variation in (h/a) , as is seen in Figure 10a.

4. Conclusions

The boundary effect and the presence of a nearby particle on the electrophoretic behavior of a particle are examined simultaneously by considering the electrophoresis of two identical spheres along the axis of a cylindrical pore under the conditions of low surface potential and weak applied electric field. The influences of the key parameters of the system under consideration, including the separation distance between two spheres, the thickness of double layer, the ratio (particle radius/pore radius), and the charged conditions on the surfaces of the spheres

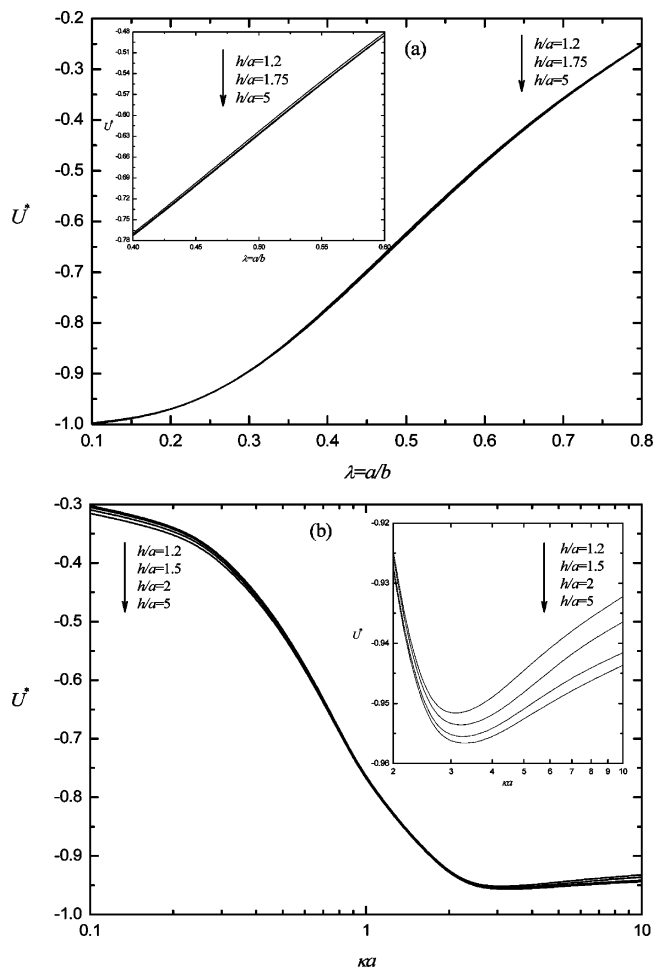


Figure 11. Variation of the scaled electrophoretic mobility, U^* , as a function of λ at various values of (h/a) at $ka = 1$ (a) and that as a function of ka at various values of (h/a) at $\lambda = 0.4$ (b). Parameters used are $\zeta_p^* = 0$ and $\zeta_w^* = 1$.

and the pore on the electrophoretic behaviors of a sphere, are discussed. For the case when two positively charged spheres are placed in a positively charged pore, we conclude the following: (a) The presence of the pore leads to results that are much more complicated than those for the case when it is absent. (b) If the boundary effect is significant, the mobility of a sphere increases monotonically with the increase in the separation distance between two spheres, and if the double layer surrounding a sphere is thin, its mobility may have a local minimum as the separation distance varies. These phenomena have not been reported for similar electrophoresis problems in the literature. (c) Similar to the case of two identical cylindrical particles with constant charge density in an uncharged cylindrical pore, the effect of particle–particle interaction on the mobility of a sphere is significant when the thickness of the double layer surrounding a sphere is thick or the boundary effect is significant. For the case when two uncharged spheres are placed in a positively charged pore, we conclude that no matter the significance of the boundary effect and the thickness of the double layer near the pore are, the mobility of a sphere increases with the increase in the separation distance between two spheres, and this effect is pronounced when the boundary effect is moderate or the thickness of the double layer is either sufficiently thin or sufficiently thick. These phenomena have not been observed for similar electrophoresis problems in the literature.

Acknowledgment. This work is supported by the National Science Council of the Republic of China.

References and Notes

- (1) Keh, H. J.; Chen, S. B. *J. Fluid Mech.* **1988**, *194*, 377.
- (2) Hsu, J. P.; Ku, M. H.; Kuo, C. C. *Langmuir* **2005**, *21*, 7588.
- (3) Hsu, J. P.; Ku, M. H.; Kao, C. Y. *J. Colloid Interface Sci.* **2004**, *276*, 248.
- (4) Shugai, A. A.; Carnie, S. L.; Chan, D. Y. C.; Anderson, J. L. *J. Colloid Interface Sci.* **1997**, *191*, 357.
- (5) Hsu, J. P.; Ku, M. H.; Kao, C. Y. *Ind. Eng. Chem. Res.* **2005**, *44*, 1105.
- (6) Read, L. D.; Morrison, F. A. *J. Colloid Interface Sci.* **1976**, *54*, 117.
- (7) Keh, H. J.; Chen, S. B. *Am. Inst. Chem. Eng. J.* **1988**, *34*, 1075.
- (8) Keh, H. J.; Chen, S. B. *J. Colloid Interface Sci.* **1989**, *130*, 542.
- (9) Keh, H. J.; Chen, S. B. *J. Colloid Interface Sci.* **1989**, *130*, 556.
- (10) Keh, H. J.; Yang, F. R. *J. Colloid Interface Sci.* **1990**, *139*, 105.
- (11) Keh, H. J.; Yang, F. R. *J. Colloid Interface Sci.* **1991**, *145*, 362.
- (12) Keh, H. J.; Chen, S. B. *J. Fluid Mech.* **1992**, *238*, 251.
- (13) Keh, H. J.; Chen, S. B. *J. Colloid Interface Sci.* **1993**, *158*, 199.
- (14) Henry, D. C. *Proc. R. Soc. London, Ser. A* **1931**, *133*, 106.
- (15) Shugai, A. A.; Carnie, S. L. *J. Colloid Interface Sci.* **1999**, *213*, 298.
- (16) Hsu, J. P.; Yeh, L. H.; Ku, M. H. *J. Colloid Interface Sci.* **2007**, *305*, 324.
- (17) Hsu, J. P.; Yeh, L. H. *J. Chin. Inst. Chem. E* **2006**, *37*, 601.
- (18) Backstrom, G. *Fluid Dynamics by Finite Element Analysis*; Studentlitteratur: Sweden, 1999.
- (19) O'Brien, R. W.; White, L. R. *J. Chem. Soc. Faraday Trans. 2* **1978**, *74*, 1607.
- (20) Hsu, J. P.; Ku, M. H. *J. Colloid Interface Sci.* **2005**, *283*, 592.
- (21) FlexPDE version 2.22, PDE Solutions Inc., U.S.A.
- (22) Stimson, M.; Jeffery, G. B. *Proc. R. Soc., A* **1926**, *111*, 110.
- (23) Happel, J.; Brenner, H. *Low Reynolds Number Hydrodynamics*; Academic Press, New York, 1983.
- (24) Ennis, J.; Anderson, J. L. *J. Colloid Interface Sci.* **1997**, *185*, 497.